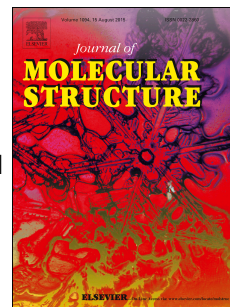


# Accepted Manuscript

Synthesis and investigation of various properties of a novel series of nonlinear optical (NLO) chromophores bearing dicyanovinyl (DCV) moiety

Nurgul Seferoğlu, Yasmina Bayrak, Ergin Yalçın, Zeynel Seferoğlu



PII: S0022-2860(17)31046-3

DOI: [10.1016/j.molstruc.2017.07.102](https://doi.org/10.1016/j.molstruc.2017.07.102)

Reference: MOLSTR 24129

To appear in: *Journal of Molecular Structure*

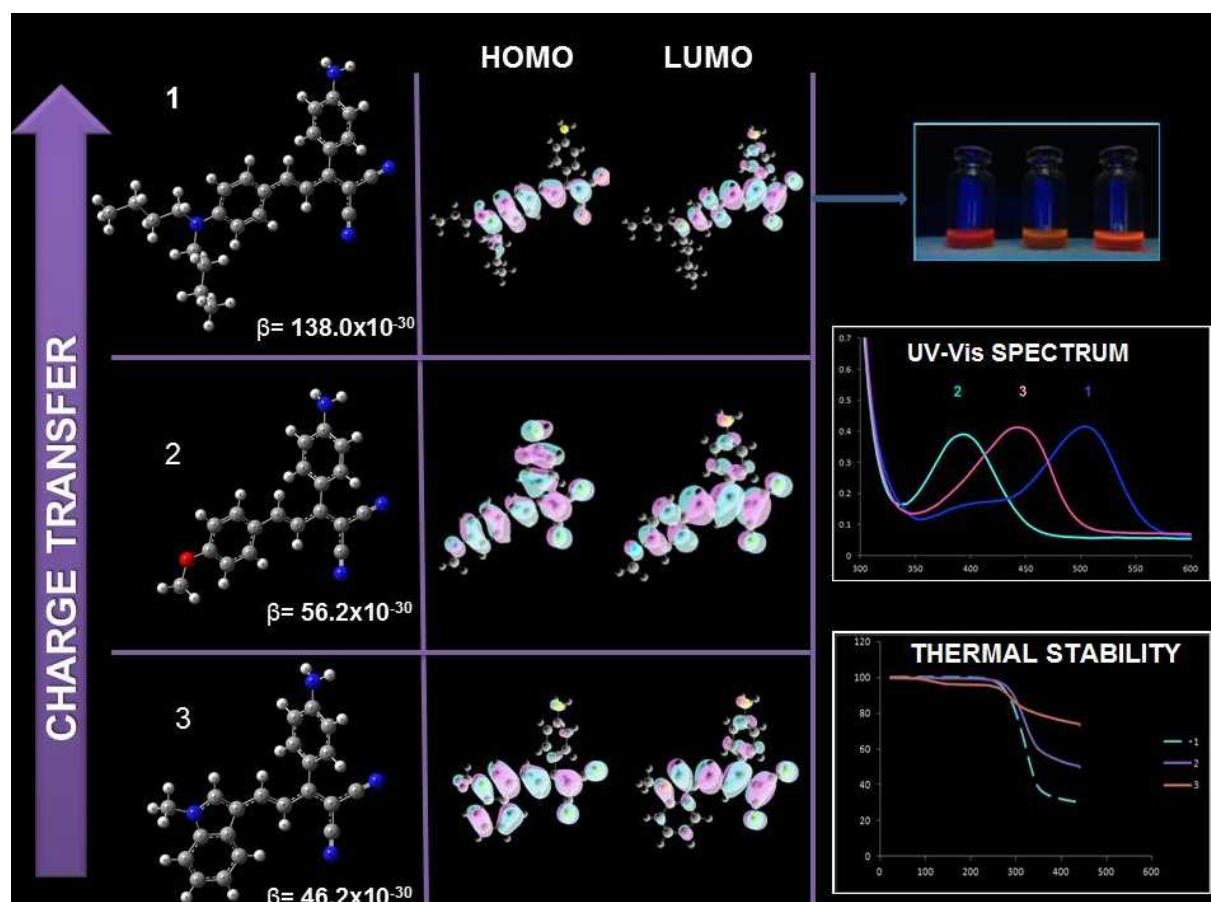
Received Date: 15 June 2017

Revised Date: 27 July 2017

Accepted Date: 29 July 2017

Please cite this article as: N. Seferoğlu, Y. Bayrak, E. Yalçın, Z. Seferoğlu, Synthesis and investigation of various properties of a novel series of nonlinear optical (NLO) chromophores bearing dicyanovinyl (DCV) moiety, *Journal of Molecular Structure* (2017), doi: 10.1016/j.molstruc.2017.07.102.

This is a PDF file of an unedited manuscript that has been accepted for publication. As a service to our customers we are providing this early version of the manuscript. The manuscript will undergo copyediting, typesetting, and review of the resulting proof before it is published in its final form. Please note that during the production process errors may be discovered which could affect the content, and all legal disclaimers that apply to the journal pertain.



**Synthesis and investigation of various properties of a novel series of nonlinear optical (NLO) chromophores bearing dicyanovinyl (DCV) moiety**

Nurgul Seferoğlu<sup>a\*</sup>, Yasmina Bayrak<sup>b</sup>, Ergin Yalçın<sup>b</sup>, Zeynel Seferoğlu<sup>b\*</sup>

<sup>a</sup>*Gazi University, Advanced Technologies, 06500 Ankara, Turkey*

<sup>b</sup>*Gazi University, Department of Chemistry, 06500 Ankara, Turkey*

**Abstract**

A series of new nonlinear optic (NLO) chromophores containing a dimethine (vinyl) as  $\pi$ -bridge and electron acceptor dicyanomethine and different electron-donating groups and heterocyclic rings were synthesized. The structures of synthesized dyes were characterized by Fourier Transform Infrared (FTIR), proton and carbon nuclear magnetic resonance ( $^1\text{H}/^{13}\text{C}$  NMR) and mass spectrometry. Their electronic absorption spectra were evaluated in MeOH, THF and DCM. The absorption maxima exhibited little bathochromic shifts for each dye with the increasing dielectric constants of the solvents. The synthesized dyes can absorb in the range of 354-506 nm. The analysis of the electronic spectra showed that the dyes having electron-donating groups or heterocyclic rings showed significant changes relative to the model dye which has no substituent on the phenyl ring. In addition, the absorption maxima moved to the longest wavelength for dye containing *N,N*-dibutylamino substituent. Experimental absorption wavelengths for the compounds were found to be in good agreement with those predicted using the Time-Dependent Density Functional Theory (TD-DFT) [B3LYP/6-311+g(d,p)]. Furthermore, the second order NLO responses of

the dyes were calculated using density functional theory (DFT) calculations. The study reveals that the synthesized chromophores have large first hyperpolarizability ( $\beta$ ) values, hence they may have potential applications in the development of NLO materials. For determination of the thermal behaviors of the compounds, thermogravimetric analysis (TGA) were done. The result showed that all the chromophores exhibited good thermal stabilities with the decomposition temperatures ( $T_d$ ) greater than 260 °C.

*Keywords:* Organic Chromophores, UV-vis, Fluorescence, Nonlinear optic (NLO) properties, donor-acceptor, density functional theory (DFT).

\*Corresponding authors Tel.: +90 312 202 3726, +90 312 202 1525

\*E-mail addresses: [nurguls@gazi.edu.tr](mailto:nurguls@gazi.edu.tr), [znseferoglu@gazi.edu.tr](mailto:znseferoglu@gazi.edu.tr)

## 1. Introduction

Recently, the design and obtaining of new NLO materials including D- $\pi$ -A structure have received interest. The structure of donor/acceptor substituents, groups or rings is very important as well as  $\pi$ -linker as a good candidate for application as an NLO molecule [1]. These groups contribute to photophysical and electrochemical properties of a molecule with reduction of energy gap between HOMO and LUMO orbitals [2-15]. In addition, NLO response becomes stronger and faster with increasing  $\pi$ -conjugation in a compound. Until now, many compounds that have been synthesized and offered as potential NLO

active compounds have dimethine bridge/bridges as linker, a dicyanovinyl (DCV) group, due to its very strong electron-attracting group and dialkylamino groups, as strong electron-donating group [1] (Scheme 1).

**Scheme 1 is here**

Compounds having dimethine bridge, especially, have also found area of usage as functional dyes in donor/acceptor systems, emission material in OLED, fluorescence probe for detection of biological molecules, and sensitizers in DSSC [16-25]. Moreover, they can also be used as NLO dyes, anion, cation chemosensors and biosensor [26]. In our previous study, we reported the NLO properties of a novel series of styryl-based push-pull chromophores as well as their optical and thermal stabilities, experimentally and theoretically [27]. In our current study, a new additional series, including the dicyanovinyl group with electron-donating groups and aromatic/heteroaromatic rings were designed, to propose as NLO candidates.

The target NLO chromophores (**3-8**) were obtained by Knoevenagel condensation of various aldehydes with **1** (Scheme 2). The structures of the compounds were characterized by spectroscopic techniques such as FTIR,  $^1\text{H}/^{13}\text{C}$  NMR and LCMS analysis. However, compound **2** was synthesized and characterized in our previous paper [27]. The photophysical properties were investigated in various solvents with different polarities. The determination of

thermal stability of the compounds was done by thermogravimetric analysis (TGA). DFT/TD-DFT computational methods were employed to rationalize the experimental data. Moreover, the second order NLO responses of the dyes were calculated by DFT computational method.

## 2. Experimental Section

### 2.1. General Instrumentations and Materials

All the chemicals used in this study were purchased from Sigma-Aldrich, and were used as such without any further purification. Thin-layer chromatography was carried out using precoated aluminium-backed plates (Merck Silica Gel 60 F254) and visualised under UV light ( $\lambda=254\text{-}365\text{ nm}$ ). FT-IR (ATR) Spectra were recorded on a Perkin Elmer 100 FT-IR spectrometer ( $\nu$  are in  $\text{cm}^{-1}$ ). NMR spectra were run on either a Bruker Avance 300 MHz, or on a 400 MHz instrument. Samples were referenced against DMSO- $d_6$  at 39.52 ppm for  $^{13}\text{C}$  and against tetramethylsilane (TMS) at 0.00 ppm for  $^1\text{H}$ . Coupling constant ( $J$ ) are given in hertz (Hz). Signals are abbreviated as follows: singlet, s; doublet, d; doublet-doublet, dd; triplet, t; multiplet, m. Chemical shifts ( $\delta$ ) are given in parts permillion (ppm) using the residue solvent peaks as reference relative to TMS. Mass analysis was obtained by using Waters 2695 Alliance ZQ Micromass LCMS working with ESI apparatus; in  $m/z$  (rel. %) (Department of Pharmacological Sciences, Ankara University Laboratories). The microwave syntheses were carried out in a Milestone Start microwave reaction system. The

melting points were measured using Electrothermal IA9200 apparatus and are uncorrected. Thermal analyses were performed with a Shimadzu DTG-60H system, up to 500 °C (10 °C min<sup>-1</sup>) under a dynamic nitrogen atmosphere (15 mL min<sup>-1</sup>). Fluorescence spectra were recorded on HITACHI F-7000 FL Spectrofluorophotometer in the range of the same solvents with a slit width of 2.5 nm used for both excitation and emission.

## 2.2. Computational details

The geometrical structures of compounds **3-8** were obtained in gas phase using different solvents by density functional theory (DFT) method at B3LYP/6-311+g(d,p) level [28]. The vibrational analysis was performed using the same method to verify as to whether the optimized structures correspond to local minima on the energy surface. For calculations within the solvents, the polarized continuum model (PCM) was used. Absorption spectra were computed using the time-dependent DFT (TD-DFT) at the same level [29] for the lowest 15 singlet-singlet transitions. The first static hyperpolarizability ( $\beta_{\text{tot}}$ ) and its related properties were also calculated. All calculations were performed using the Gaussian 09 package [30].

### 2.3 The synthesis of starting compound **1**

Compound **1** was synthesized and characterized using our previous published methods [27].

### 2.4. General procedures for the synthesis of NLO chromophores (**3-8**) by the reaction with appropriate aldehyde and compound **1**.

A mixture of 2-(1-(4-aminophenyl)ethylidene)malononitrile (**1**) (366 mg, 2 mmol), appropriate aldehyde (2 mmol) and a few drops piperidine in 20 mL ethanol was stirred over night under reflux. After cooling to room temperature, a solid precipitate formed. The precipitate was filtered off and then recrystallized using 50 % (v:v) of ethanol-water mixture to obtain a pure compound.

#### **(E)-2-((1-(4-aminophenyl)-3-(4-methylphenyl)allylidene)malononitrile (**3**)**

The crude product was recrystallized from ethanol-water mixture as yellow solid. Yield 44% (125 mg), m.p. 212-214 °C; IR (KBr)  $\nu/\text{cm}^{-1}$ : 3464, 3370, 3211, 2208, 1628  $\text{cm}^{-1}$ ;  $^1\text{H}$  NMR (DMSO- $d_6$ , 300 MHz):  $\delta$  7.61 (d,  $J = 8.1$  Hz, 2H),  $\delta$  7.40 (d,  $J_{\text{trans}} = 15.6$  Hz, 1H),  $\delta$  7.31 (d,  $J = 8.7$  Hz, 2H),  $\delta$  7.29 (d,  $J = 8.1$ , 2H),  $\delta$  7.08 (d,  $J_{\text{trans}} = 15.6$  Hz, 1H),  $\delta$  6.69 (d,  $J = 8.6$  Hz, 2H),  $\delta$  6.20 (s, 2H),  $\delta$  2.32 (s, 3H) ppm;  $^{13}\text{C}$  NMR (CDCl<sub>3</sub>, 100 MHz):  $\delta$  171.2, 153.8, 148.2, 141.9, 132.6,



132.4, 130.3, 129.2, 124.3, 119.7, 116.1, 115.2, 113.6, 74.63, 74.6, 21.6 ppm;

LC-MS (m/e) , (M-H)<sup>+</sup> calculated for C<sub>19</sub>H<sub>15</sub>N<sub>3</sub> found: 286.34 calc.: 286.35.

**(E)-2-((1-(4-aminophenyl)-3-(4-methoxyphenyl)allylidene)malononitril (4)**

The crude product was recrystallized from ethanol-water mixture as yellow solid. Yield 52% (155 mg), m.p. 170-172 °C; IR (KBr)  $\nu/\text{cm}^{-1}$ : 3458, 3356, 2212, 1585  $\text{cm}^{-1}$ ; <sup>1</sup>H NMR (DMSO-*d*<sub>6</sub>, 300 MHz):  $\delta$  7.68 (d, *J* = 8.8 Hz, 2H),  $\delta$  7.31 (d, *J*<sub>trans</sub> = 15.5 Hz, 1H),  $\delta$  7.29 (d, *J* = 8.6 Hz, 2H),  $\delta$  7.07 (d, *J*<sub>trans</sub> = 16.1 Hz, 1H),  $\delta$  7.01 (d, *J* = 8.9 Hz, 2H),  $\delta$  6.68 (d, *J* = 8.7 Hz, 2H),  $\delta$  6.17 (s, 2H),  $\delta$  3.81 (s, 3H) ppm; <sup>13</sup>C NMR (DMSO-*d*<sub>6</sub>, 100 MHz):  $\delta$  171.5, 162.3, 153.2, 148.3, 131.6, 129.1, 127.8, 122.7, 120.1, 115.3, 115.2, 114.6, 113.6, 73.9, 55.7 ppm; LC MS (m/e) , (M+H)<sup>+</sup> calculated for C<sub>19</sub>H<sub>15</sub>N<sub>3</sub>O found: 302.24 calc.: 302.35.

**(E)-2-((1-(4-aminophenyl)-3-(4-dibuthylaminophenyl)allylidene)malononitril (5)**

The crude product was recrystallized from ethanol-water mixture as bright dark green solid. Yield 50% (198 mg), m.p. 170-173 °C; IR (KBr)  $\nu/\text{cm}^{-1}$ : 3468, 3362, 3245, 2954, 2926, 2864, 2214, 1605  $\text{cm}^{-1}$ ; <sup>1</sup>H NMR (DMSO-*d*<sub>6</sub>, 300 MHz):  $\delta$  7.49 (d, *J* = 8.6 Hz, 2H),  $\delta$  7.20 (d, *J* = 8.6 Hz, 2H),  $\delta$  7.13 (d, *J*<sub>trans</sub> = 15.1 Hz, 1H),  $\delta$  6.95 (d, *J*<sub>trans</sub> = 15.1 Hz, 1H),  $\delta$  6.69 (d, *J* = 9.2 Hz, 2H),  $\delta$  6.68 (d, *J* = 8.7

Hz, 2H), 6.00 (s, 2H), 1.51 (m, 4H), 1.31 (m, 4H) 0.9 (t, 6H) ppm;  $^{13}\text{C}$  NMR (DMSO- $d_6$ , 100 MHz):  $\delta$  171.6, 153.1, 151.1, 149.8, 132.1, 131.9, 121.7, 120.2, 118.3, 116.8, 116.0, 113.6, 112.1, 70.7, 50.4, 29.5, 20.1, 14.3 ppm; LC MS (m/e),  $(\text{M}+\text{H})^+$  calculated for  $\text{C}_{26}\text{H}_{30}\text{N}_4$  found: 399.49 calc.: 399.55.

**(E)-2-(1-(4-aminophenyl)-3-(indole-3-yl)allylidene)malononitril (6)**

The crude product was recrystallized from ethanol-water mixture as reddish orange solid. Yield 60% (185 mg), m.p. 247-249 °C; IR (KBr)  $\nu/\text{cm}^{-1}$ : 3483, 3381, 3257, 3103, 3047, 2212, 2200, 1587  $\text{cm}^{-1}$ ;  $^1\text{H}$  NMR (DMSO- $d_6$ , 300 MHz):  $\delta$  8.10 (s, 1H),  $\delta$  7.9 (dd, 1H),  $\delta$  7.6 (dd, 1H),  $\delta$  7.36 (m, 6H),  $\delta$  6.71 (d,  $J$  = 8.6 Hz, 2H)  $\delta$  6.10 (s, 2H) ppm;  $^{13}\text{C}$  NMR (DMSO- $d_6$ , 100 MHz):  $\delta$  172.8, 153.0, 144.6, 138.4, 136.2, 132.1, 124.9, 123.8, 122.5, 120.3, 119.9, 118.7, 116.7, 116.2, 114.3, 113.6, 113.5, 70.33 ppm; LC MS (m/e),  $(\text{M}-\text{H})^+$  calculated for  $\text{C}_{19}\text{H}_{14}\text{N}_4$  found: 311.27 calc.: 311.36.

**(E)-2-(1-(4-aminophenyl)-3-(1-methylindole-3-yl)allylidene)malononitril (7)**

The crude product was recrystallized from ethanol-water mixture as orange solid. Yield 63% (205 mg), m.p. 254-256 °C; IR (KBr)  $\nu/\text{cm}^{-1}$ : 3440, 3353, 3232, 3118, 2211, 1597  $\text{cm}^{-1}$ ;  $^1\text{H}$  NMR (DMSO- $d_6$ , 300 MHz):  $\delta$  8.10 (s, 1H),  $\delta$  7.85 (dd, 1H),  $\delta$  7.6 (dd, 1H),  $\delta$  7.36 (m, 6H),  $\delta$  6.71 (d,  $J$  = 8.6 Hz, 2H)  $\delta$  6.10 (s,

2H) ppm;  $^{13}\text{C}$  NMR (DMSO- $d_6$ , 100 MHz):  $\delta$  172.6, 153.0, 143.7, 139.0, 138.8, 132.1, 125.5, 123.9, 122.7, 120.3, 119.9, 118.6, 116.8, 116.2, 113.6, 113.2, 111.9, 70.3, 33.7 ppm; LC MS (m/e) (M-H) $^+$  calculated for  $\text{C}_{20}\text{H}_{16}\text{N}_4$  found: 325.32 calc.: 325.39.

**(E)-2-(1-(4-aminophenyl)-3-(pyridine-3-yl)allylidene)malononitril (8)**

The crude product was recrystallized from ethanol-water mixture as reddish brown solid. Yield 42% (115 mg), m.p. 126-130 °C; IR (KBr)  $\nu/\text{cm}^{-1}$ : 3458, 3335, 3220, 3038, 2208, 1637, 1602  $\text{cm}^{-1}$ ;  $^1\text{H}$  NMR (DMSO- $d_6$ , 300 MHz):  $\delta$  8.85 (s, 1H),  $\delta$  8.61 (d, 1H),  $\delta$  8.22 (d,  $J = 8.05$  Hz 1H),  $\delta$  7.55 (d,  $J_{trans} = 15.8$  Hz, 1H),  $\delta$  7.49 (m, 2H)  $\delta$  7.35 (d,  $J = 8.7$  Hz, 2H),  $\delta$  7.25 (d,  $J_{trans} = 15.8$  Hz, 1H), 6.70 (d, ,  $J = 8.7$  Hz 1H)  $\delta$  6.29 (d,  $J = 8.7$  Hz 2H), ppm;  $^{13}\text{C}$  NMR (DMSO- $d_6$ , 100 MHz):  $\delta$  170.4, 154.2, 151.7, 150.7, 144.3, 135.8, 132.9, 130.9 , 127.2, 124.3, 119.5, 115.5, 114.0, 113.4, 75.4 ppm; LC MS (m/e) , (M-H) $^+$  calculated for  $\text{C}_{17}\text{H}_{12}\text{N}_4$  found: 273.18 calc.: 273.31.

### 3. Results and Discussion

#### 3.1. Preparation of push-pull based NLO chromophores

The structures of synthesized dyes are seen in **Figure 1**. The dyes were prepared via coupling reaction between the aldehydes bearing various donor groups and 2-(1-(4-aminophenyl)ethylidene)malononitrile (**1**). In the synthetic pathway, 2-(1-(4-aminophenyl)ethylidene)malononitrile (**1**) was prepared in high yield (92%) by the reaction of 4-aminoacetophenone with malononitrile, using microwave irradiation (MWI) (**Scheme 2**). The obtained 2-(1-(4-aminophenyl)ethylidene)malononitrile (**1**) was then condensed with the appropriate aldehydes in ethanol using catalytic amounts of piperidine to afford NLO candidate dyes (**3-8**) in moderate yields as 50, 52, 44, 63, 60 and 42%, for (**3**, **4**, **5**, **6**, **7** and **8**) respectively. All the compounds were obtained with Knoevenagel reaction. Compound **2**, which was synthesized in our previous study [27], was used as model compound while evaluating the photophysical and NLO properties of dyes **3-8**.

The structures of compounds **3-8** were confirmed by spectroscopic methods such as FT-IR,  $^1\text{H}/^{13}\text{C}$  NMR, as well as by the use of LC-MS spectrometry. The spectral data were consistent with the proposed structures (**Supplementary material Figs. S1-24**). The synthesized dyes have vinylic bond as spacer and can show *E-Z* stereoisomerization. The  $^1\text{H}$  NMR spectra of all the compounds

showed that the compounds are stable as *E* stereoisomer according to vinilic coupling constant values ( $J_{\text{HH}} = 15\text{--}16$  Hz) of the olefinic protons.

**Scheme 2 is here**

**Figure 1 is here**

### 3.2. Molecular geometry optimizations

The optimized structures of the compounds **3-8** were obtained in the gas phase (**Fig.2**) and in different solvents by using DFT method at the B3LYP/6-311+g(d,p) level. The comparison of the geometry parameters was given with respect to **2** [27] used as a reference compound (**Fig. 2**). When the bond lengths of **3-8** were compared with the bond lengths of **2**, it was seen that there was no significant changes, but only the changes in C1-C2 bond lengths with the values 0.027 Å and 0.025 Å for compounds **6** and **7**, respectively. This resulted from the indole and *N*-methyl indole rings in **6** and **7**, in which the unpaired electron pair on the nitrogen atom delocalized to the ring, thereby strengthening the bonding electrons.

**Figure 2 is here**

As mentioned in the introduction, the donor-acceptor structure in conjugate molecule is important for increasing NLO response. As a result of this structure, an intramolecular charge transfer (ICT) was expected to be occurring, and increasing the strength of donor-acceptor groups as well as the planarity arrangement of these groups. In our studied molecules, the planarity of aromatic/heteroaromatic ring,  $\pi$ -bridge and dicyanomethine group are provided with a small twisting. Twisting values between the dicyanomethine acceptor and the aromatic/heteroaromatic groups are  $-13.4^\circ$ ,  $-15.1^\circ$ ,  $-15.5^\circ$ ,  $-11.9^\circ$ ,  $-11.6^\circ$ ,  $-16.3^\circ$ , for **3-8**, respectively. The C16-C14-C13-C24 dihedral in compounds **3-8** is around  $50^\circ$ , indicating that the 4-aminophenyl ring is not coplanar with the rest of the molecule. Detailed information is given in **Table 1**.

**Table 1 is here**

### 3.3. Photophysical properties

The theoretical and experimental absorption properties of the dyes were studied in three different solvents having different dielectric constants ( $\epsilon$ ). The solvents employed for the photophysical studies were; methanol (MeOH,  $\epsilon=32.70$  Debye), tetrahydrofuran (THF,  $\epsilon=7.58$  Debye) and dichloromethane (DCM,  $\epsilon=8.93$  Debye). The absorption spectra of **3-8** were recorded over the  $\lambda_{\max}$  range of (300-800 nm) and the analyses were carried out using low concentrations of

solutes ( $1 \times 10^{-5}$  M). The results of these investigations are summarized in **Table 2**. In calculations, the absorption wavelength of the compounds were calculated at the ground state structure, in each solvents, using TD-DFT (B3LYP) with the 6-311+G(d,p).

### Table 2 is here

When the absorption maxima ( $\lambda_{\max}$ ) of all compounds **3-8** were compared with the reference **2**, it was observed that, both the electron donor groups (**3-5**) and aromatic/heteroaromatic rings (**6-8**), their  $\lambda_{\max}$  values were affected in all the solvents used, and their  $\lambda_{\max}$  shifted to higher wavelengths (**Fig.3**). Thus, their bathochromic shifts were observed with increasing donor strength of substituents or rings. As expected, the biggest bathochromic shift was observed for **3** because of *N,N*-dibutylamino substituent that has stronger electron donating property than the other substituents (**Fig. 4**). Hence, an ICT in **3** would be larger than the rest of the compounds. As a result of increasing ICT in a molecule, the largest NLO response could be expected for **3**. A discussion on this is given in the following section. However, absorption maxima changes slightly in more polar MeOH with respect to DCM in the range 2-7 nm for **3-6**, 14-25 nm for **7** and **8** as indicated in **Table 2**. For example, in DCM, all the synthesized compounds, except for **8**, showed absorption wavelengths ( $\lambda_{\max}$ ) in the visible region. The absorption spectra of the dyes **3**, **4**, **6** and **7**, in DCM

showed one intense broad band and a maximum centered at around 394 nm, 413 nm, 422 nm, 427 nm and 488 nm, respectively. This major absorption band can be assigned to the combined ICT transition, from electron donor groups or ring, to the dicyanomethine acceptor.

Chromophore **3** has *N,N*-dibutylamino group acting as strong donor group and in this molecule, the ICT is very effective to be evaluated in push-pull system. Comparing the three electron-donating groups in the synthesized compounds, the ICT increases in the order  $\text{CH}_3 < \text{OCH}_3 < \text{NBU}_2$ , in accordance with the electron-donating ability of these substituents.

**Figure 3 and 4 are here**

On the other hand, interestingly, only **3** had fluorescence properties, even under UV light, as shown in photograph in **Fig.5**. The emission property of **3** was studied in one protic (MeOH) and two aprotic solvents (DCM and THF) of various polarity. Compound **3** showed a blue-shifted fluorescence emission maxima, in DCM, that is less polar with respect to methanol. The effect of solvent polarities on emission behavior of **3** is shown in **Fig.6**. The result showed that with the increasing of solvent polarity, bathochromic shift were observed in emission band of **3**. Therefore, it can be said that the compound **3** exhibit positive fluorosolvatochromism.



**Figure 5 and 6 are here**

### *3.4. Molecular Orbitals*

To understand the electronic transition and charge delocalization within these push-pull chromophores, different molecular orbitals were also studied. According to our TD-DFT calculations, the main absorption bands with the largest oscillator strengths were found to correspond to the electronic transition from the highest occupied molecular orbital (HOMO) to the lowest unoccupied molecular orbital (LUMO), and from HOMO-1 to the LUMO, with different contributions for all the studied compounds (**Table 2**). The shapes of these orbitals and the energies are given in the **Fig.7 and Table 3**. While the HOMO and LUMO energies increased for the donor-substituted Compounds **3, 4, 5, 6, and 7**, and decreased for compound **8**, the energy gap ( $\Delta E_{H \rightarrow L}$ ) increased for **4, 5, 6, and 7**, and decreased for the other compounds as compared to **2** (**Table 3**). Comparison of solvent effects on  $\Delta E_{H \rightarrow L}$  values indicated small changes with increasing solvent polarity. At the same time, the smallest  $\Delta E_{H \rightarrow L}$  value was obtained for **3** having the largest molecular chain length among the studied molecules.

### 3.5. Nonlinear optic (NLO) properties

The NLO properties of the designed and synthesized dyes **3-8**, to be presented as NLO candidates, were investigated using DFT calculations. The data obtained for polarizability ( $\alpha$ ), first hyperpolarizability ( $\beta$ ), and electronic dipole moment ( $\mu$ ) with their components, as shown in **Table 4**, show that, **2** has smaller  $\beta$  value ( $26.1 \times 10^{-30}$  esu) and **3** has larger  $\beta$  value ( $138.0 \times 10^{-30}$  esu) than the other studied compounds. The obtained  $\beta$  values for **4-8** were found to be greater than that of **2**, with the values 56.2, 35.3, 46.2, 39.7, and  $32.0 \times 10^{-30}$  esu, respectively. After comparison of  $\beta$  values of **3-8** with **2**, it was seen that, the presence of heterocyclic rings, in place of phenyl or electron-donor groups at para position of phenyl ring, resulted in greater NLO property. On the other hand, the strength of their electron donating groups changed as follows: **3** > **4** > **5**. According to this, **3** showed greater NLO response due to it has stronger electron donating group (*N,N*-dibutylamino). Urea is usually used as a reference compound in the investigation of NLO properties of molecular systems. The  $\beta$  value of urea was obtained as  $0.61 \times 10^{-30}$  esu by B3LYP/6-311+G(d,p). The obtained  $\beta$  values of the investigated molecules were greater than urea by 60 and 230 times. These dyes, for having large hyperpolarizability, can be used as a promising candidate in the field of NLO. As seen in **Table 4**,  $\beta_{\text{xyy}}$  component is more predominated for **8**, but for all other compounds,  $\beta_{\text{xxx}}$  component is dominated. Having a

certain dominant component means that there is a significant charge transfer in this direction.

### 3.6. Thermal properties

Decomposition temperature ( $T_d$ ) values for chromophores generally increase with the increase in conjugation length, and electron rich substituent effect. High molecular weight and polar substituents of organic chromophores are vital for intermolecular interactions, such as van der Waals force and dipole-dipole interaction, and increases thermal stability. In addition, since thermal stability is very important for chromophore applications in NLO devices, therefore NLO chromophores must be thermally stable enough to withstand high temperatures ( $>200^\circ\text{C}$ ) in electric field poling and subsequent processing of chromophore/polymer materials [25]. This is because some processes for the preparation of NLO devices are carried out at high temperature. In this study, in order to investigate the thermal stability of the chromophores, thermogravimetric analysis (TGA) was used. The change in weight of each of the compounds was measured as a function of temperature. All the chromophores exhibited good thermal stabilities with the decomposition temperatures ( $T_d$ ) higher than  $240^\circ\text{C}$  ( $262\text{--}302^\circ\text{C}$ ). Compound **6** had the highest  $T_d$  value ( $302^\circ\text{C}$ ), followed by **3** ( $283^\circ\text{C}$ ), **4** ( $274^\circ\text{C}$ ), **5** ( $262^\circ\text{C}$ ), **7**

(268 °C), and **8** (267 °C), as shown in **Fig. 8**. Hence, all the thermal stabilities of the six chromophores are enough for application in EO device preparation.

### 3. Conclusion

In this paper, a series of novel dye-based second NLO chromophores has been synthesized and their structures were confirmed by FT-IR,  $^1\text{H}$  NMR,  $^{13}\text{C}$  NMR as well as LCMS spectra. All the chromophores have an *E*-configuration of the vinylic double bond as unequivocally shown by  $^1\text{H}$  NMR spectroscopy. The optical properties of the dyes were studied in various solvents of different polarities. Bathochromic shift was observed with strong electron-donating group and increasing ICT. The biggest bathochromic shift was observed in **3** because of *N,N*-dibutylamino substituent that has more strong electron donor property. At the same time, compound **3** had fluorescent properties in various solvents.

In addition, the chromophores were optimized using B3LYP/6-311+G (d,p) level in ground state geometry. The geometrical parameters and electronic spectra were discussed. The dyes have shown a prominent absorption at the longer wavelength due to HOMO→LUMO transition with high oscillator strength. Moreover, NLO properties have been investigated theoretically and found that the dyes demonstrate a large second-order nonlinear response and this is mainly due to the strong  $\pi$ -conjugation. The TGA results show that they have a good thermal stability.

In conclusion, the synthesized dyes can be used as promising candidates for various applications in NLO, electronic and photonic devices.

## Acknowledgements

We are grateful to The Scientific and Technological Research Council of TURKEY for providing financial support (Project Grant No: 114F296) for this study.

## References

- [1] Z. Seferoğlu, Recent Synthetic Methods for the Preparation of Charged and Uncharged Styryl-based NLO Chromophores: A Review, Organic Preparations and Procedures International, 1–44, (2017), in press, DOI: 10.1080/00304948.2017.1336052.
- [2] J.Y. Lee, H.B. Bang, T.S. Kang, E.J. Park, Molecular design, synthesis and electrooptic properties of novel Y-type polyurethanes with high thermal stability of second harmonic generation, Eur. Polym. J. 40(8) (2004) 1815-22.
- [3] B.J. Coe, S.P. Foxon, E.C. Harper, M. Helliwell, J. Raftery, C.A. Swanson, Evolution of linear absorption and nonlinear optical properties in V-shaped ruthenium(II)-based chromophores, J. Am. Chem. Soc. 132(5) (2010) 1706-23.
- [4] I. Fuks-Janczarek, J.M. Nunzi, B. Sahraoui, I.V. Kityk, J. Berdowski, A.M.

Caminade, Third-order nonlinear optical properties and two-photon absorption in branched oligothiénylenevinylenes, *Opt. Commun.* 209(4-6) (2002) 461-6.

[5] Q. Li, C. Lu, J. Zhu, E. Fu, C. Zhong, S. Li, Y. Cui, J. Qin, Z. Li, Nonlinear optical chromophores with pyrrole moieties as the conjugated bridge: enhanced NLO effects and interesting optical behavior, *J. Phys. Chem. B.* 112(15) (2008) 4545-4551.

[6] X.H. Zhou, J. Davies, S. Huang, J.D. Luo, Z.W. Shi, B. Polishak, Y. Cheng, T. Kim, L. Johnson, A. Jen Facile structure and property tuning through alteration of ring structures in conformationally locked phenyltetraene nonlinear optical chromophores, *J. Mater. Chem.* 21(12) (2011) 4437-4444.

[7] W. Gong, Q. Li, Z. Li, C. Lu, J. Zhu, S. Li, J. Yang, Y. Cui, J. Qin, Synthesis and characterization of indole-containing chromophores for second-order nonlinear optics, *J. Phys. Chem. B.* 110(21) (2006) 10241-10247.

[8] H. Kang, G. Evmenenko, P. Dutta, K. Clays, K. Song, T.J. Marks, X-shaped electrooptic chromophore with remarkably blue-shifted optical absorption. synthesis, characterization, linear/nonlinear optical properties, self-assembly, and thin film microstructural characteristics, *J. Am. Chem. Soc.* 128(18) (2006) 6194-6205.

[9] S.R. Marder, Organic nonlinear optical materials: where we have been and where we are going, *Chem. Commun.* 2 (2006) 131–134.

[10] S. Bo, C. Hu, F. Huo, F. Liu, J. Liu, X. Liu, L. Qiu, H. Wang, Y. Yang, Z. Zhen, Comparative studies on structure nonlinearity relationships in a series of

novel second-order nonlinear optical chromophores with different aromatic amine donors, *Dyes and Pigments*. 120 (2015) 347-356.

[11] S. Achelle, A. Barsella, C. Baudequin, B. Caro, F.J. Robin-Le Guen, Synthesis and Photophysical Investigation of a Series of Push–Pull Arylvinyldiazine Chromophores, *J. Org. Chem.* 77 (2012) 4087-4096.

[12] Z. Guo, W. Zhu, H. Tian, Dicyanomethylene-4H-pyran chromophores for OLED emitters, logic gates and optical chemosensors, *Chem. Commun.* 48 (2012) 6073–6084.

[13] N.J. Long, Organometallic compounds for nonlinear optics-The search for En-lightenment, *Angewandte Chemie International Edition in English*. 34 (1995) 21–38.

[14] M.G. Kuzyk, Using fundamental principles to understand and optimize nonlinear-optical materials, *J. Mater. Chem.* 19 (2009) 7444–7465.

[15] S. Dabek, J. Heck, T. Meyer-Friedrichsen, H. Wong, Mono- and dinuclear sesquifulvalene complexes, organometallic materials with large nonlinear optical properties, *Coord. Chem. Rev.* 190 (1999) 1217–1254.

[16] T. Chau Van, C. Dhenaut, I. Ledoux, J. Zyss, Harmonic rayleigh scattering from nonlinear octupolar molecular media: the case of crystal violet, *Chem. Phys.* 177 (1993) 281-296;

[17] I. Ledoux, J. Zyss, Nonlinear optics in multipolar media: theory and experiments, *Chem. Rev.* 94 (1994) 77-105.

[18] P. Kaatz, D.P. Shelton, Spectral measurements of hyper-Rayleigh light

scattering, *Rev. Sci. Instrum.* 67 (1996) 1438; P. Kaatz, D.P. Shelton, Polarized hyper-Rayleigh light scattering measurements of nonlinear optical chromophores, *J. Chem. Phys.* 105 (1996) 3918.

[19] K. Clays, L. De Maeyer, A. Persoons, *Advances in Chemical Physics*. Ed: M. Evans, S. Kielich, Wiley, New York, 1994.

[20] K. Clays, A. Persoons, Hyper-Rayleigh scattering in solution, *Phys. Rev. Lett.* 66 (1991) 2980-2983.

[21] H. Zollinger, *Color Chemistry, Synthesis, Properties and Applications of Organic Dyes and Pigments*, third ed., Wiley-VCH, 2003.

[22] G. Wu, F. Kong, J. Li, W. Chen, C. Zhang, Q. Chen, X. Zhang, S. Dai, Julolidine dyes with different acceptors and thiophene-conjugation bridge: Design, synthesis and their application in dye-sensitized solar cells, *Synthetic Metals*. 180 (2013) 9–15.

[23] H. Hu, C. Liu, Y. Liu, Y. Liu, D. Zhang, Theoretical investigation on second-order nonlinear optical properties of (dicyanomethylene)-pyran derivatives, *J. Mol. Struct.* 570 (2001) 43-51.

[24] D.R. Kanis, M.A. Ratner, T.J. Marks, Design and construction of molecular assemblies with large second-order optical nonlinearities. Quantum chemical aspects, *Chem. Rev.* 94 (1994) 195-242.

[25] C. Hu, F. Liu, H. Zhang, F. Huo, Y. Yang, H. Wang, , H. Xiao, Z. Chen, J. Liu, L. Qiu, Z. Zhen, X. Liu, S. Bo, Synthesis of novel nonlinear optical chromophores: achieving excellent electro-optic activity by introducing benzene



derivative isolation groups into the bridge, J. Mater. Chem. C. 3 (2015) 11595-11604.

[26] T. Deligeorgiev, A. Vasilev, S. Kaloyanova and J.J. Vaquero, Styryl dyes-synthesis and applications during the last 15 years, Color. Technol., 126, (2010), 55-80.

[27] S. Achelle, A.Barsella, Y. Bayrak, N. Seferoğlu, Z. Seferoğlu, E. Yalçın, Styryl-based NLO chromophores: Synthesis, spectroscopic properties and theoretical calculations, Tet. Lett. 56 (2015) 2586-2589.

[28] (a) C.T. Lee, W.T. Yang, R.G. Parr, Phys. Rev. B. 37 (1988) 785-789; (b) A.D. Becke, J. Chem. Phys. 98(7) (1993) 5648-5652. c) P.C. Hariharan, J.A. Pople, Theor. Chem. Acc. 28 (1973) 213-222.

[29] R. Bauernschmitt, R. Ahlrichs, Chem. Phys. Lett. 256 (1996) 454-464.

[30] M.J. Frisch, G.W. Trucks, H.B. Schlegel, G.E. Scuseria, M.A. Robb, J.R. Cheeseman, , et al., Gaussian 09 revision C01, Wallingford CT: GaussianInc, 2010.

## CAPTIONS

## Tables Captions

**Table 1.** Obtained from ground state geometry in gas phase, selected bond lengths (Å), bond angle (°) and dihedral angle (°) values for **2-8**.

**Table 2.** Obtained maximum wavelength values from the absorption spectrum for **2-8**.  $\lambda_{max}^{exp}$ : experimental values,  $\epsilon$ : molar absorption coefficient,  $\lambda_{max}^{cal}$ : calculated values and f: oscillator strength. H and L, respectively, HOMO and LUMO orbitals.

**Table 3.** Calculated orbital energy values in the gas phase and different solvent for **2-8**. Values are eV unit.

**Table 4.** Polarizability ( $\alpha$ ) and its  $\alpha$ -components, first hyperpolarizability ( $\beta$ ) and its  $\beta$ -components and dipole moment calculated at B3LYP/6-311+g(d,p) level for **2-8**.

## Scheme Captions

**Scheme 1.** Some well-known NLO candidate chromophores bearing DCV moiety.

**Scheme 2.** Synthetic pathway of **3-8**.

## Figure Captions

**Fig.1.** Chemical structure of chromophores **2-8**.

**Fig.2.** Optimized geometry parameters of **2-8** in gas phase. Bond lengths are in Å and angles are in degree. **2** is used as a reference compound [27].

**Fig.3.** UV-vis spectra of **3-8** in MeOH, THF and DCM with various dielectric constants ( $\epsilon$ ) ( $c=1\times10^{-5}$ ).

**Fig.4.** UV-vis spectra of compounds **2-8** in DCM ( $c=1\times10^{-5}$ ).

**Fig.5.** Picture of Fluorescence color changes of **3** in MeOH, THF and DCM solutions ( $c=1\times10^{-5}$ ;  $\lambda_{\text{ex}}=365$  nm). The picture was taken in the dark upon irradiation with UV lamp.

**Fig.6.** Fluorescence emission spectra of chromophore **3** ( $1\times10^{-6}$ ) in different solvents.

**Figure 7.** Calculated molecular orbitals in gas phase for compounds **2-8**.

**Fig. 8.** TGA curves of **3-8**.

**Table 1.** Obtained from ground state geometry in gas phase, selected bond lengths (Å), bond angle (°) and dihedral angle (°) values for **2-8**.

Compound	2	5	4	3	7	6	8
<i>Bond length</i>							
C1-C2	1.459	1.445	1.453	1.456	1.432	1.434	1.457
C1-C11	1.353	1.361	1.356	1.354	1.361	1.359	1.352
C11-C13	1.449	1.440	1.445	1.448	1.440	1.442	1.452
C13-C14	1.478	1.481	1.479	1.478	1.482	1.482	1.476
C13-C24	1.384	1.389	1.386	1.385	1.388	1.387	1.384
C21-N30	1.386	1.389	1.387	1.386	1.389	1.388	1.384
C24-C25	1.426	1.425	1.425	1.426	1.425	1.425	1.426
C24-C26	1.428	1.426	1.427	1.427	1.426	1.426	1.427
C25-N27	1.157	1.157	1.157	1.157	1.157	1.157	1.157
C26-N28	1.157	1.157	1.157	1.157	1.158	1.157	1.157
<i>Bond angle</i>							
C1-C11-C13	126.8	127.1	127.1	126.9	127.6	127.6	126.4
C11-C13-C24	119.1	119.6	119.3	119.2	119.6	120.5	118.9
C14-C13-C24	120.4	119.8	120.1	120.2	119.8	119.8	120.6
C13-C24-C25	123.2	123.2	123.2	123.2	123.2	123.1	123.2
C24-C25-N27	177.8	177.9	177.9	177.9	178.0	178.0	177.8
C24-C26-N28	179.6	179.5	179.5	179.6	179.2	179.2	179.5
C19-C21-N30	120.8	120.8	120.8	120.8	120.8	120.8	120.8
C25-C24-C26	115.2	115.4	115.3	115.2	115.5	115.5	115.2
<i>Dihedral angle</i>							
C2-C1-C11-C13	-178.9	-179.3	-178.8	-178.8	-179.1	-179.1	-178.8
C1-C11-C13-C24	165.9	167.9	166.9	166.4	168.5	168.4	165.3
C11-C13-C14-C16	128.2	126.8	127.1	127.6	125.6	125.5	129.0
C16-C14-C13-C24	-51.9	-53.4	-52.9	-52.4	-54.5	-54.5	-51.0

**Table 2.** Obtained maximum wavelength values from the absorption spectrum for **2-8**.  $\lambda_{max}^{exp}$ : experimental values,  $\epsilon$ : molar absorption coefficient,  $\lambda_{max}^{cal}$ : calculated values and f: oscillator strength. H and L, respectively, HOMO and LUMO orbitals.

Compounds	MeOH		THF		DCM	
	$\lambda_{max}^{ex.}$ (nm) ( $\epsilon, 10^3 \text{ Lmol}^{-1} \cdot \text{cm}^{-1}$ )	$\lambda_{max}^{cal.}$ (nm) (f)	$\lambda_{max}^{ex.}$ (nm) ( $\epsilon, 10^3 \text{ Lmol}^{-1} \cdot \text{cm}^{-1}$ )	$\lambda_{max}^{cal.}$ (nm) (f)	$\lambda_{max}^{ex.}$ (nm) ( $\epsilon, 10^3 \text{ Lmol}^{-1} \cdot \text{cm}^{-1}$ )	$\lambda_{max}^{cal.}$ (nm) (f)
<b>2</b>	354 (59.5),	380(0.939) H-1→L(96.6%) H→L(2.8%)	355 (65.4),	381(0.968) H-1→L(95.8%) H→L (3.4%)	357 (64.1),	382(0.971) H-1→L(95.9%) H→L (3.2%)
<b>3</b>	501 (38.9)	489(1.2084) H-1→L(11.9%) H→L(88.1%)	490 (50.7)	486.39(1.2308) H-1→L(10.3%) H→L(89.6%)	506 (41.6)	488(1.2389) H-1→L(10.5%) H→L (89.0%)
<b>4</b>	392 (38.4)	416(1.002) H-1→L(85.6%) H→L(14.0%)	392 (39.3)	416(1.0295) H-1→L(76.6%) H→L(22.9%)	396 (39.1)	413(1.0275) H-1→L(82.1%) H→L(17.5%)
<b>5</b>	365 (27.0)	393(1.019) H-1→L(94.9%) H→L(4.4%)	367 (34.3)	393(1.047) H-1→L(93.8%) H→L(5.5%)	372 (39.5)	394(1.050) H-1→L(94.1%) H→L(5.2%)
<b>6</b>	447 (44.6)	425(0.6975) H-1→L(26.6%) H→L(71.9%)	438 (53.7)	425(0.6879) H-1→L(24.3%) H→L(74.4%)	445 (41.3)	427(0.6842) H-1→L(26.2%) H→L(72.5%)
<b>7</b>	441 (30.1)	421(0.7394) H-1→L(9.0%) H→L(89.4%)	430 (28.5)	420(0.7630) H-1→L(4.1%) H→L(94.3%)	427 (16.7)	422(0.7613) H-1→L(5.3%) H→L(93.2%)
<b>8</b>	443 (13.7)	376(0.6696) H-1→L(98.6%)	440 (14.5)	374(0.7082) H-1→L(98.2%)	418 (13.3)	375(0.7113) H-1→L(98.3%)

All spectra were recorded at room temperature in the concentration  $1.0 \times 10^{-5}$  M.

**Table 3.** Calculated orbital energy values in the gas phase and different solvent for **2-8**. Values are eV unit.

	Gaz fazı	MeOH	THF	CH <sub>2</sub> Cl <sub>2</sub>	Gaz fazı	MeOH	THF	CH <sub>2</sub> Cl <sub>2</sub>
	<b>2</b>				<b>3</b>			
H-1	-6.655	-6.598	-6.602	-6.601	-6.058	-6.050	-6.043	-6.044
H	-6.274	-6.113	-6.135	-6.130	-5.570	-5.546	-5.546	-5.545
L	-3.035	-3.069	-3.060	-3.062	-2.607	-2.817	-2.778	-2.786
$\Delta E_{H \rightarrow L}$	3.239	3.044	3.075	3.068	2.963	2.729	2.768	2.759
$\Delta E_{H-1 \rightarrow L}$	3.620	3.530	3.541	3.539	3.451	3.233	3.265	3.258
	<b>4</b>				<b>5</b>			
H-1	-6.302	-6.186	-6.193	-6.214	-6.502	-6.440	-6.443	-6.442
H	-6.127	-6.089	-6.096	-6.121	-6.221	-6.102	-6.118	-6.115
L	-2.867	-2.969	-2.949	-2.943	-2.953	-3.022	-3.007	-3.010
$\Delta E_{H \rightarrow L}$	3.260	3.120	3.147	3.178	3.268	3.080	3.111	3.105
$\Delta E_{H-1 \rightarrow L}$	3.435	3.217	3.244	3.271	3.549	3.418	3.436	3.432
	<b>6</b>				<b>7</b>			
H-1	-6.153	-6.059	-6.066	-6.065	-6.199	-6.069	-6.084	-6.081
H	-5.841	-5.862	-5.854	-5.856	-5.958	-5.952	-5.949	-5.949
L	-2.600	-2.751	-2.721	-2.727	-2.663	-2.782	-2.757	-2.762
$\Delta E_{H \rightarrow L}$	3.241	3.111	3.133	3.129	3.295	3.170	3.192	3.187
$\Delta E_{H-1 \rightarrow L}$	3.553	3.308	3.345	3.338	3.536	3.287	3.327	3.319
	<b>8</b>							
H-1	-6.893	-6.796	-6.810	-6.807				
H	-6.368	-6.129	-6.161	-6.154				
L	-3.221	-3.165	-3.173	-3.172				
$\Delta E_{H \rightarrow L}$	3.147	2.964	2.988	2.982				
$\Delta E_{H-1 \rightarrow L}$	3.672	3.631	3.637	3.635				

**Table 4.** Polarizability ( $\alpha$ ) and its  $\alpha$ -components, first hyperpolarizability ( $\beta$ ) and its  $\beta$ -components and dipole moment calculated at B3LYP/6-311+g(d,p) level for **2-8**.

Compound	2	3	4	5	6	7	8
$\alpha_{xx}$	380.25	680.35	459.62	426.49	475.29	445.706	391.91
$\alpha_{xy}$	19.07	-34.04	20.82	21.04	21.97	16.6001	3.97
$\alpha_{yy}$	311.33	404.88	318.08	317.73	363.43	342.850	277.37
$\alpha_{xz}$	-7.97	-13.72	-8.15	-7.88	-8.18	-6.913	-6.91
$\alpha_{yz}$	2.26	-18.43	1.51	2.10	0.74	2.291	-3.56
$\alpha_{zz}$	140.33	227.94	151.62	149.09	163.70	154.057	140.716
$\alpha$ (esu)	<b>41.1x10<sup>-24</sup></b>	<b>64.9x10<sup>-24</sup></b>	<b>45.9x10<sup>-24</sup></b>	<b>44.1x10<sup>-24</sup></b>	<b>49.5x10<sup>-24</sup></b>	<b>46.6x10<sup>-24</sup></b>	<b>40.4x10<sup>-24</sup></b>
$\mu_x$	-0.70	8.69	-4.22	-3.25	-4.34	-2.56	-1.23
$\mu_y$	-3.42	-7.67	-6.78	-7.82	-10.51	-10.33	-3.65
$\mu_z$	0.15	1.44	1.04	0.73	0.62	0.40	0.29
$\mu$ (D)	<b>8.87</b>	<b>11.68</b>	<b>8.06</b>	<b>8.50</b>	<b>11.39</b>	<b>10.65</b>	<b>9.81</b>
$\beta_{xxx}$	1998.27	-17375.1	6812.35	4047.09	5440.79	3748.09	172.37
$\beta_{xyx}$	1981.07	2819.84	2618.79	2030.47	2956.97	3164.68	2866.66
$\beta_{xyy}$	-1453.53	1759.89	-1490.11	-1544.17	-1111.90	-667.52	1418.44
$\beta_{yyy}$	1095.51	1177.92	1169.92	1272.95	353.07	311.95	538.34
$\beta_{xxz}$	25.59	-99.64	77.24	49.01	-25.43	56.15	68.506
$\beta_{xyz}$	32.26	-414.77	2.31	8.24	48.31	63.54	44.24
$\beta_{yyz}$	0.49	-225.97	-27.67	-7.48	-71.13	-49.28	15.65
$\beta_{zzz}$	-18.83	101.44	14.25	11.99	-59.22	-7.63	-1.20
$\beta_{yzz}$	-98.55	-39.58	-63.61	-83.03	-82.33	-59.53	-60.30
$\beta_{zzz}$	0.30	46.99	22.49	3.45	17.07	19.39	11.78
$\beta$ (esu)	<b>26.1x10<sup>-30</sup></b>	<b>138.0x10<sup>-30</sup></b>	<b>56.2x10<sup>-30</sup></b>	<b>35.3x10<sup>-30</sup></b>	<b>46.2x10<sup>-30</sup></b>	<b>39.7x10<sup>-30</sup></b>	<b>32.0x10<sup>-30</sup></b>

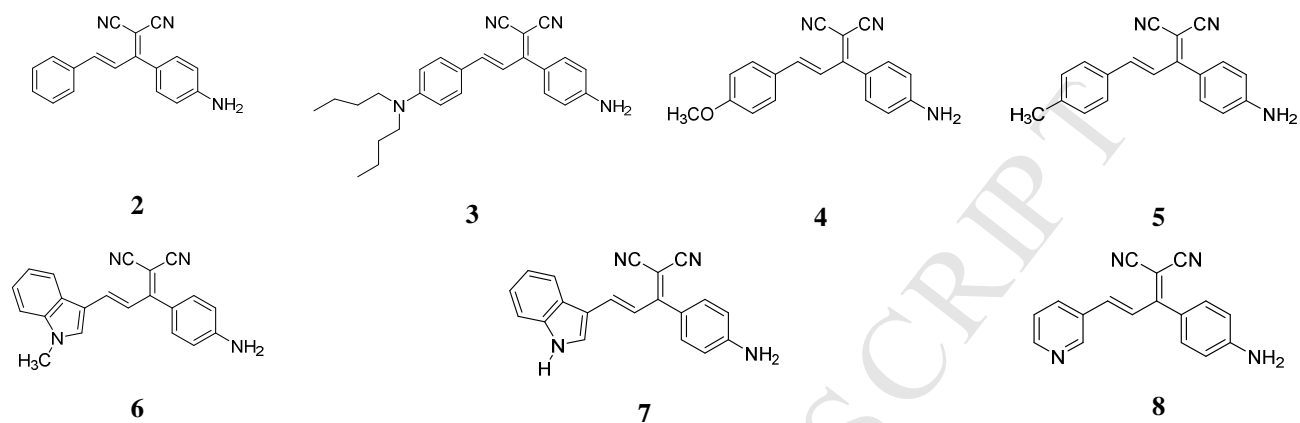


**Fig.1.** Chemical structure of chromophores 2-8.





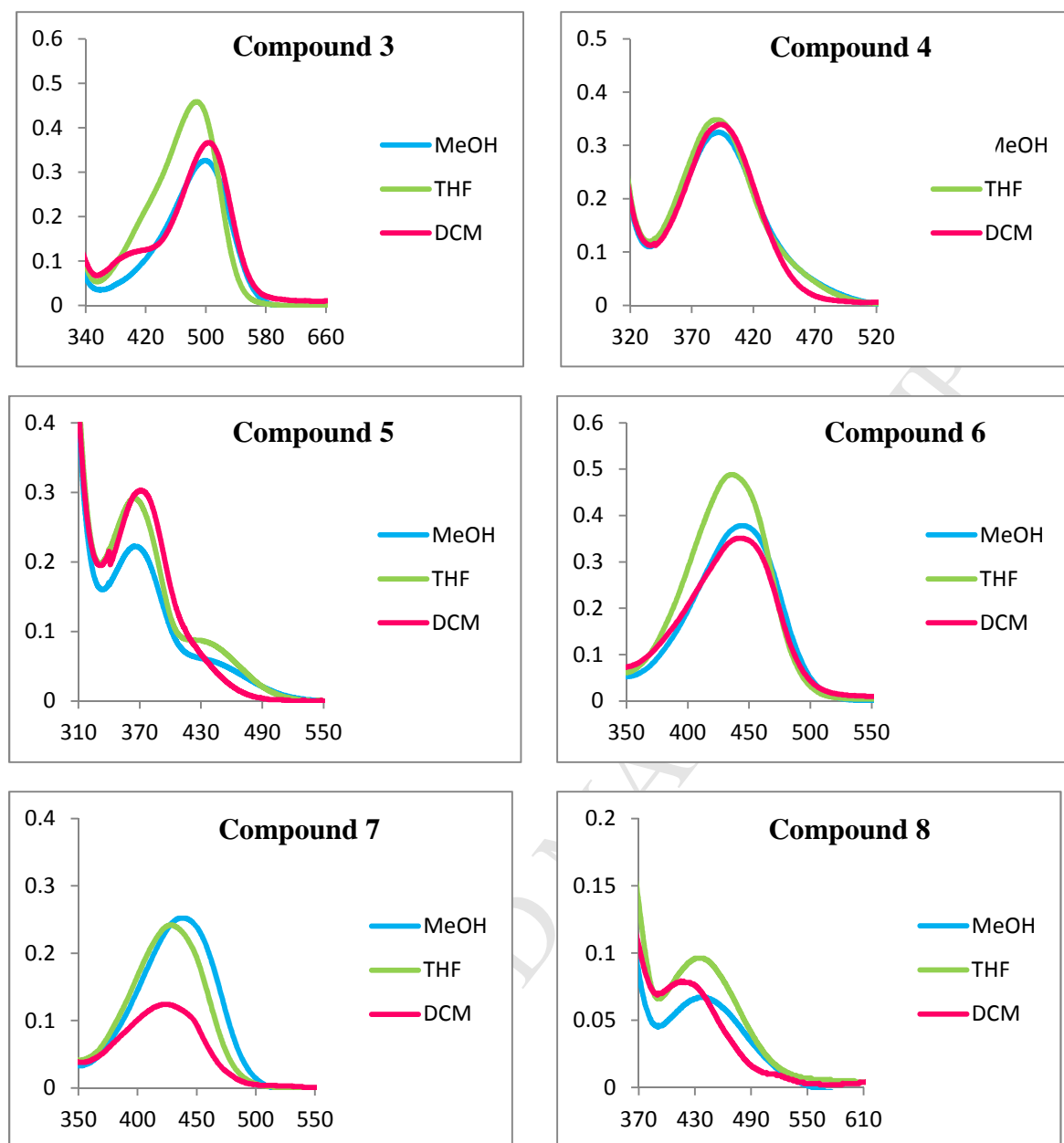


**Fig.3.** UV-vis spectra of **3-8** in MeOH, THF and DCM with various dielectric constants ( $\epsilon$ ) ( $c=1 \times 10^{-5}$ ).

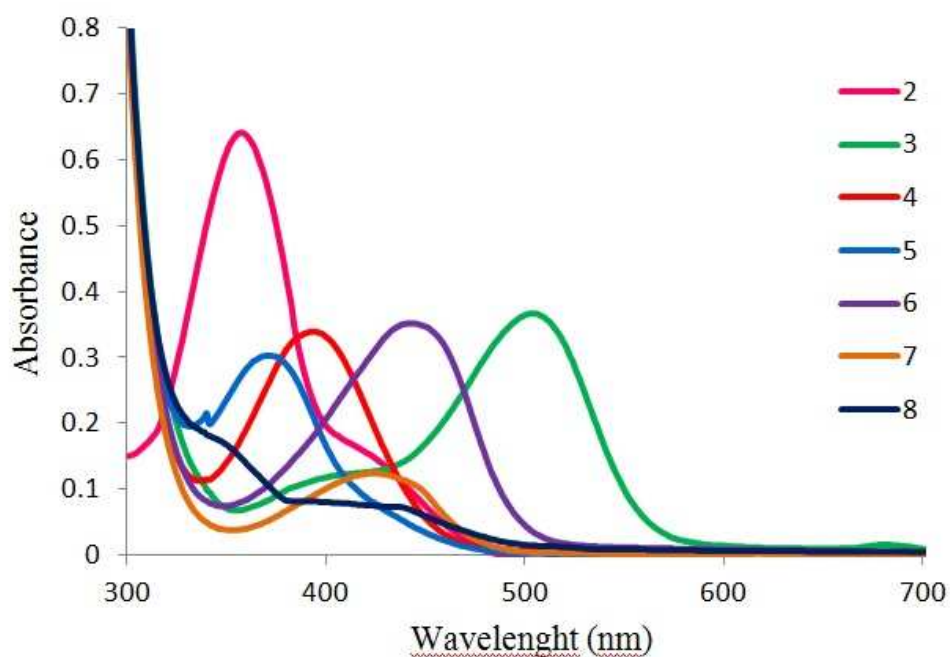


**Fig.4.** UV-vis spectra of compounds **2-8** in DCM ( $c=1 \times 10^{-5}$ ).

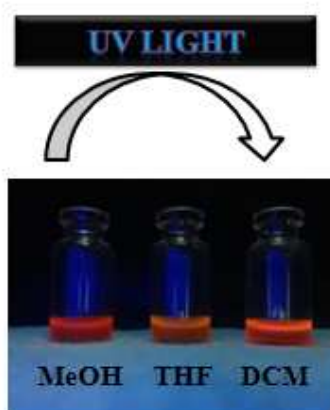


**Fig.5.** Picture of Fluorescence color changes of **3** in MeOH, THF and DCM solutions ( $c=1 \times 10^{-5}$ ;  $\lambda_{\text{ex}}=365$  nm). The picture was taken in the dark upon irradiation with UV lamp.

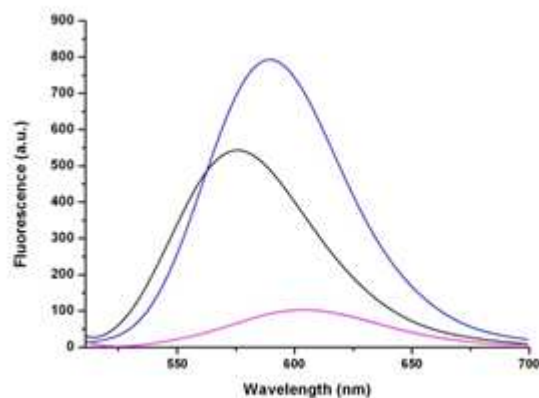


**Fig.6.** Fluorescence emission spectra of chromophore **3** ( $1 \times 10^{-6}$ ) in different solvents (THF (black ), DCM (blue), MeOH (pink)).

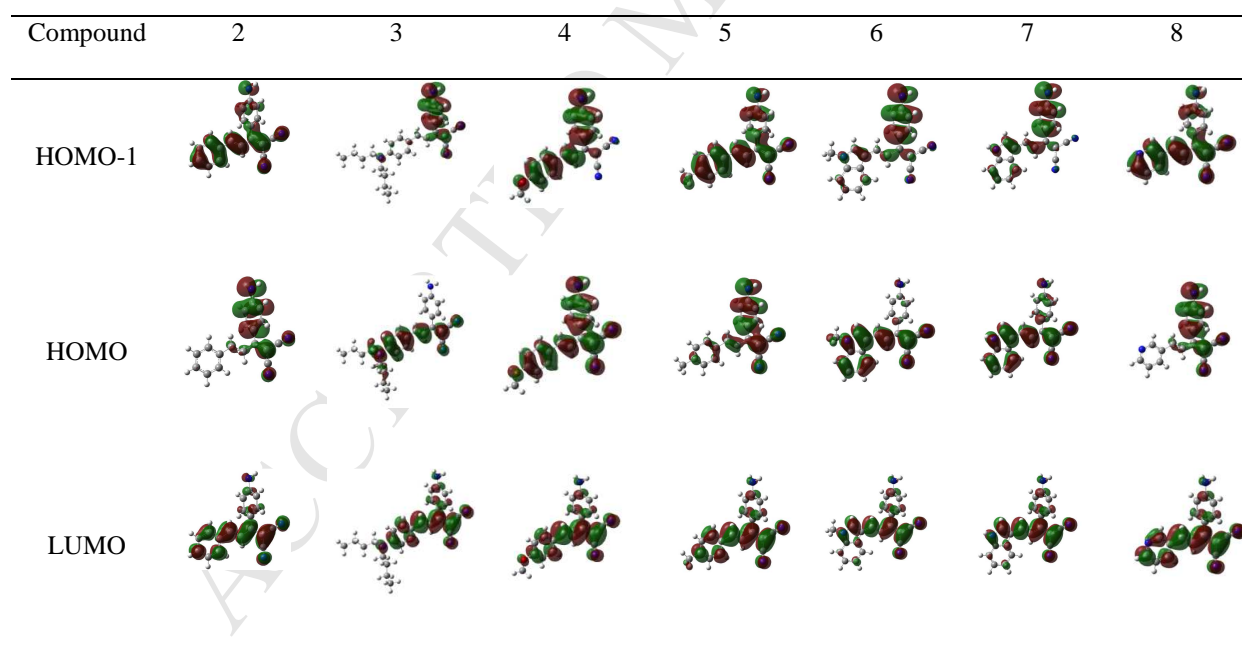


**Figure 7.** Calculated molecular orbitals in gas phase for compounds **2-8**.

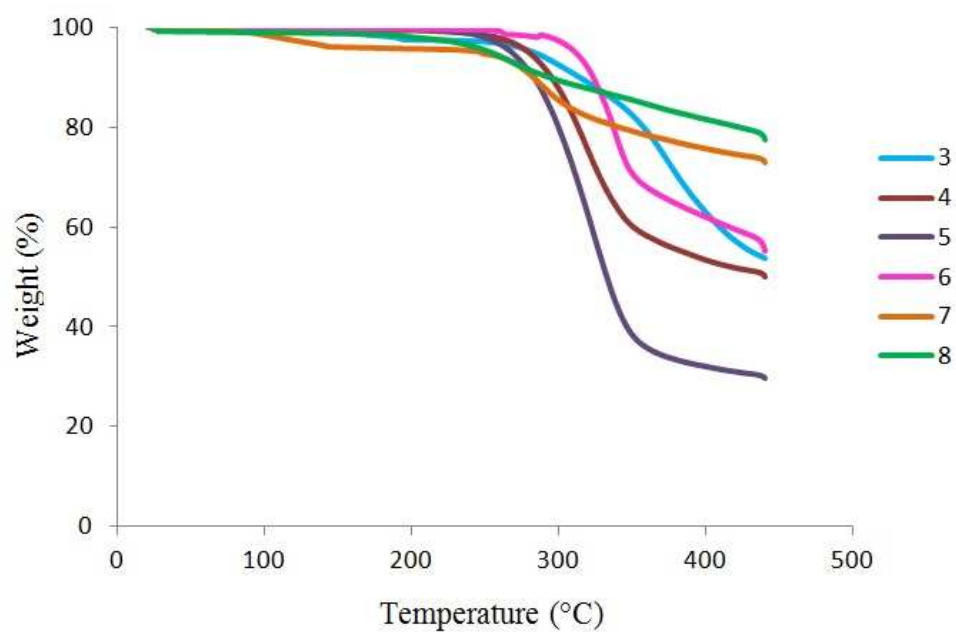
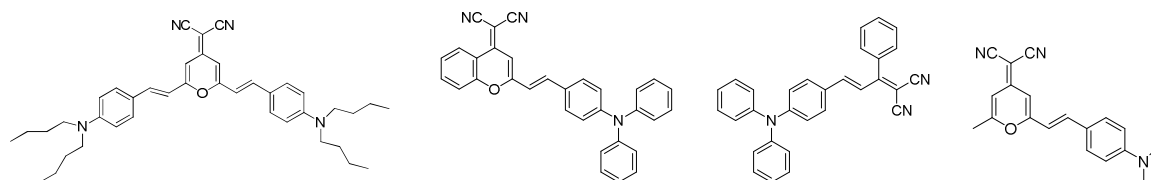
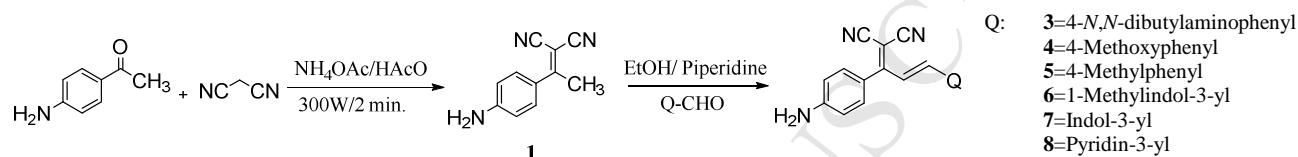


**Fig. 8.** TGA curves of **3-8**.



**Scheme 1.** Some well-known NLO candidate chromophores bearing DCV moiety.



**Scheme 2.** Synthetic pathway of **3-8**.

**Highlights**

- A new series NLO chromophores were synthesized and characterized.
- The maximum absorption values of the dyes in the range of 354-506 nm.
- The introduction of *N,N*-dibutylamino substituent into the para position of phenyl ring increase ICT with observing bathochromic shift.
- The dye having *N,N*-dibutylamino has fluorescence property.
- They showed good thermal stability for practical applications as NLO dye.